DNA interactions and anticancer screening of copper(II) complexes of N-*(methylpyridin-2-yl)-amidino-O-methylurea*

Romrawee Pratumwieng, Atittaya Meenongwa, Rosa F. Brissos, Patrick Gamez, Yanee Trongpanich & Unchulee Chaveerach

Transition Metal Chemistry

ISSN 0340-4285
Volume 42
Number 4

Transit Met Chem (2017) 42:311-322
DOI 10.1007/s11243-017-0134-z

Springer

Transit Met Chem (2017) 42:311–322
DOI 10.1007/s11243-017-0134-z

DNA interactions and anticancer screening of copper(II) complexes of *N*-(methylpyridin-2-yl)-amidino-*O*-methylurea

Romrawee Pratumwieng[1] · Atittaya Meenongwa[2] · Rosa F. Brissos[3] · Patrick Gamez[3,4] · Yanee Trongpanich[5] · Unchulee Chaveerach[1]

Received: 4 December 2016 / Accepted: 6 March 2017 / Published online: 21 March 2017

Abstract Cu(II) complexes of the tridentate ligand *N*-(methylpyridin-2-yl)-amidino-*O*-methylurea (L), namely $[Cu(L)Cl_2]$ and $[Cu(L)ClO_4]ClO_4$, have been investigated for interactions with DNA by spectroscopic methods and viscosity measurements. Both complexes bind to DNA through non-intercalative interactions. $[Cu(L)Cl_2]$ ($K_b = 2.81 \times 10^5\ M^{-1}$) shows similar DNA-binding potential to $[Cu(L)ClO_4]ClO_4$ ($K_b = 1.57 \times 10^5\ M^{-1}$). Investigation of the chemical nuclease properties toward plasmid pBR322 DNA by gel electrophoresis and atomic force microscopy (AFM) suggests that both complexes are able to cleave the supercoiled form (Form I) to the nicked (Form II) and linear forms (Form III) through an oxidative pathway. The possible reactive oxygen species have been investigated by the use of scavengers, indicating that hydroxyl radicals may be involved in the DNA cleavage mechanism. Both of these complexes show similar activities against selected human cancer cell lines.

Introduction

The synthesis of molecules which can bind to DNA and/or show nuclease properties has received much attention in recent years [1–3]. Investigations of the interactions of DNA with metal complexes provide a basis to develop novel pharmaceuticals. Transition metal complexes have been widely exploited for these purposes, not only because of their distinctive spectral and electrochemical properties, but also due to the fact that by changing the ligand environment one can tune the interactions of such complexes with DNA. Platinum-based drugs such as cisplatin have dominated the treatment of various cancers. The design of new metal complexes that can interact with DNA requires a detailed understanding of how platinum and other metals interact and process DNA.

In recent years, copper(II) complexes have received much interest for the development of new drugs and molecular probes for DNA [4, 5]. Additionally, some copper(II) compounds have been found to possess antimicrobial [6–8] and antitumor [8, 9] activities. In the present work, we have investigated the biological activities of two copper(II) complexes of *N*-(methylpyridin-2-yl)-amidino-*O*-methylurea (L), namely $[Cu(L)Cl_2]$ and $[Cu(L)ClO_4]ClO_4$ (Fig. 1). These complexes were previously prepared and structurally characterized by our research group [10]. The *N*,*N*,*N*-tridentate ligand (L) is a guanidine derivative; such compounds are of considerable interest owing to their high potential for hydrogen-bond-mediated interactions [11]. Additionally, naturally occurring or synthetic

Electronic supplementary material The online version of this article (doi:10.1007/s11243-017-0134-z) contains supplementary material, which is available to authorized users.

✉ Unchulee Chaveerach
sunchul@kku.ac.th

[1] Department of Chemistry and Center of Excellence for Innovation in Chemistry, Faculty of Science, Materials Chemistry Research Center, Khon Kaen University, Khon Kaen 40002, Thailand

[2] Chemistry Division, Department of Science, Faculty of Science and Technology, Rajamangala University of Technology Krungthep, Bangkok 10120, Thailand

[3] Departament de Química Inorganica, Universitat de Barcelona, Martí I Franquès 1-11, 08028 Barcelona, Spain

[4] Institució Catalana de Recerca I Estudis Avançats (ICREA), Passeig Lluís Companys, 23, 08010 Barcelona, Spain

[5] Department of Biochemistry, Faculty of Science, Khon Kaen University, Khon Kaen 40002, Thailand

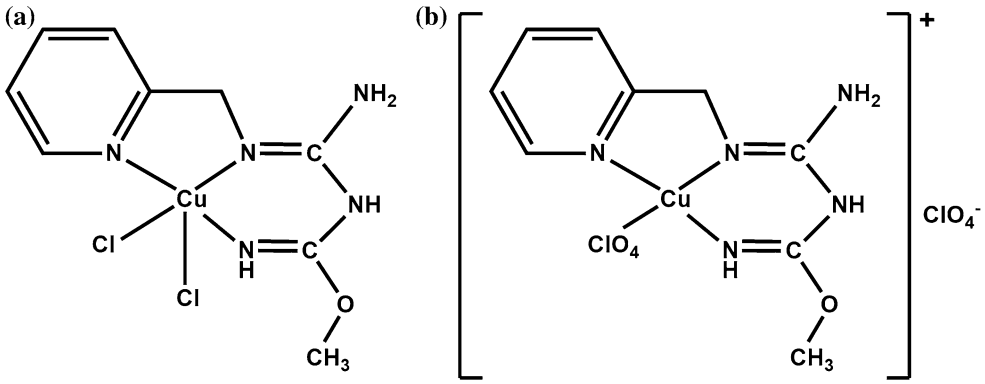

Fig. 1 Structures of $[Cu(L)Cl_2]$ (**a**) and $[Cu(L)ClO_4]ClO_4$ (**b**) used in this work [10, 15]

compound-containing guanidine groups have been reported to possess a wide range of biological activities, including anticancer, antimicrobial, antiviral, antibiotic, and anti-inflammatory properties [12, 13]. Recently, we have reported the nucleobase-binding capabilities of $[Cu(L)Cl_2]$ and $[Cu(L)ClO_4]ClO_4$ toward adenine, cytosine, guanine and thymine [14]. They also exhibit binding potential toward a model DNA nucleotide, 5′-guanosine monophosphate (5′-GMP), and possess antibacterial activity against three human-food-poisoning bacteria [14]. These observations suggest that both complexes are potential DNA-interacting agents and could find applications in cancer treatment.

In the current work, the DNA-binding capabilities of $[Cu(L)Cl_2]$ and $[Cu(L)ClO_4]ClO_4$ have been studied with calf thymus (CT) DNA using absorption titration, viscosity measurements, thermal denaturation experiments, competitive DNA-binding studies, circular dichroism spectroscopy and stoichiometric determination. Their nuclease activities toward plasmid pBR322 DNA were also investigated by gel electrophoresis and atomic force microscopy (AFM). Furthermore, their in vitro anticancer activities were tested against three human cancer cell lines, specifically MCF-7 (breast cancer), NCI-H187 (small cell lung cancer), and KB (oral cavity cancer), by resazurin microplate assay (REMA).

Experimental

Materials and instrumentation

Disodium salt of calf thymus DNA (CT-DNA, Type I fibrous) was purchased from Sigma-Aldrich. Plasmid pBR322 DNA was obtained from Vivantis. Ethidium bromide (EB) solution (10 mg mL^{-1}) and tris(hydroxylmethyl)aminomethane (Tris base) were obtained from Promega. Agarose (D-1, Low EEO) was purchased from Pronadisa. DMSO and *t*-BuOH were purchased from Riedel-Haën and Univar, respectively. KI, glycerol, MeOH, and NaN_3 were obtained from Sigma-Aldrich. All reagents were of molecular biology grade and used as received. $[Cu(L)Cl_2]$ and $[Cu(L)ClO_4]ClO_4$ were prepared by the previously reported procedure [10, 15].

Electronic absorption spectra were recorded using an Agilent 8453 UV–visible spectrophotometer. Fluorescence determinations were performed on a Shimadzu RF-5301PC spectrofluorophotometer. Circular dichroism (CD) spectra were recorded on a Jasco J-810 spectropolarimeter. The amount of Cu for determination of the stoichiometry was determined with a Perkin Elmer AAnalyst 100 atomic absorption spectrometer. Electrophoretic band intensities were visualized with a Bio-Rad Gel Doc 2000 system using Lab Work software. AFM images were obtained using a Nanoscope V Multimode 8 AFM (Bruker AXS) operating in the PEAK FORCE tapping mode. Commercial Si-tip on nitride lever cantilevers (SNL, Bruker) with a force constant of 0.4 N m^{-1} were used.

DNA-binding studies

The DNA stock solution, prepared in Tris buffer (containing 5 mM Tris–HCl and 50 mM NaCl at pH 7.1), gave a UV absorbance ratio A_{260}/A_{280} of 1.8–1.9 (where A_{260} and A_{280} are the absorbances of a DNA sample at 260 and 280 nm, respectively), indicating that the DNA was sufficiently free of protein concentration [16]. The DNA stock solution was kept at 4 °C and used within 4 days. A tenfold dilution of the DNA was determined spectrophotometrically at 260 nm by using the molar extinction coefficient value of 6600 M^{-1} cm^{-1} [17]. All experiments were carried out in Tris buffer at pH 7.1 in sterile deionized water.

Electronic absorption titrations

Absorption titration experiments were performed by varying the CT-DNA concentration from 0 to 30 μM, while keeping the metal complex concentration constant at 50 μM in Tris buffer. All samples were incubated at 37 °C for 24 h. Their absorption titration data were recorded in the range of 200–400 nm, using Tris buffer as a blank. In

order to evaluate the DNA-binding strengths of the complexes, the intrinsic binding constants (K_b) were determined using the following equation [18];

$$[DNA]/(\varepsilon_a - \varepsilon_f) = [DNA]/(\varepsilon_b - \varepsilon_f) + 1/K_b(\varepsilon_b - \varepsilon_f) \quad (1)$$

where [DNA] is the concentration of DNA, ε_a is given by A_{obsd}/[Cu], ε_f and ε_b are the extinction coefficient of the free metal complex and the complex in fully bound form, respectively. In the plot of [DNA]/($\varepsilon_a - \varepsilon_f$) versus [DNA], the K_b value is given by the ratio of slope to the y intercept.

Fluorescence spectroscopy

Emission intensity measurements were carried out using a spectrofluorophotometer. CT-DNA (100 μM) was pretreated with an equimolar amount of EB and left for 15 min at room temperature in the dark. The complex was then added to this mixture in [Complex]/[DNA] (r) ratios of 0.0–1.0 with 0.2 intervals, and left in the dark for 15 min before measurement. Emission intensities were measured from 500 to 700 nm with an excitation wavelength at 500 nm. Quenching data were analyzed according to the linear Stern–Volmer equation [19];

$$F_0/F = 1 + K_{SV}[Q] \quad (2)$$

where F_0 and F represent the fluorescence intensities of the DNA-EB complex in the absence and presence of quencher, respectively. K_{sv} is the linear Stern–Volmer quenching constant and [Q] is the quencher concentration. In the plot of F_0/F versus [Complex], K_{sv} is given by the ratio of the slope to intercept.

Viscosity measurements

Viscosity measurements were carried out on an Ubbelohde viscometer, immersed in a constant temperature bath at 37.0 ± 0.1 °C. The CT-DNA concentration was kept constant (100 μM), while the complex concentration was varied in the [Complex]/[DNA] (r) ratio of 0.0–1.0 with intervals of 0.1. Flow time was measured with a digital stopwatch. Each sample was measured three times and the average flow time was calculated. The viscosity at each ratio was determined by the flow time of the DNA-containing solutions (t) corrected by the flow time of buffer alone (t_0), $\eta = t - t_0$. Data are presented as relative viscosity $(\eta/\eta_0)^{1/3}$ versus r, where η is the viscosity of DNA in the presence of the complex, and η_0 is the viscosity of DNA alone.

Circular dichroism spectroscopy

CD spectra were recorded over 220–320 nm at room temperature. All experiments were done using a quartz cell of 1 cm length and a scan rate of 100 nm min^{-1} with a response time of 4 s. The concentration of CT-DNA in Tris buffer was kept constant at 70 μM, while the complex concentration was varied over the [Complex]/[DNA] ratio of 0.5 and 1.0.

Thermal denaturation

Thermal denaturation of CT-DNA was investigated on a UV–visible spectrophotometer with Peltier temperature-controlling cell holder and increment temperature rate of 0.5 °C min^{-1}. The absorbances of CT-DNA (100 μM) in the absence and presence of each complex in [Complex]/[DNA] ratios of 0.0, 0.1, 0.2, 0.3, and 0.4 were recorded in Tris buffer. Melting curves were plotted between the relative absorption intensity (A/A_0, A_0 and A are the initial and the observed absorbances at 260 nm) and temperature range from 25 to 100 °C. The melting temperature (T_m) was determined from the maximum of the first derivative or tangentially from the graph at midpoint of the transition curves. ΔT_m is defined as the difference between the T_m values of bound and free DNA.

Stoichiometric determination

The stoichimetry of the interactions between the complexes and DNA was determined by a procedure similar to that described in the literature [20]. The CT-DNA solution (5 mM, 1 mL) was added to the complex solution (5 mM, 1 mL), and the resulting mixture was incubated for 24 h at 37 °C. Precipitation of the copper(II)/DNA complex was obtained upon adding absolute ethanol (4 mL) and aqueous NaCl (2 M, 0.2 mL). The solution containing the precipitate was stored at −70 °C for 1 h, and the precipitate was subsequently isolated by centrifugation at 4 °C (10,000 rpm, 30 min). The supernatant was separated by slow decantation. Finally, deionized water (25 mL) was added to dissolve the copper(II)/DNA precipitate, and the DNA concentration was calculated (from triplicate experiments) by the absorption intensity at 260 nm using $\varepsilon = 6600\ M^{-1}\ cm^{-1}$ [17]. The amount of copper(II) was measured by atomic absorption spectrometry (AAS), hence providing the Cu (mmol)/DNA (mol base) ratio.

Nuclease activity

Gel electrophoresis

The DNA-cleaving properties of the complexes were investigated using agarose gel electrophoresis. Plasmid pBR322 DNA (0.1 μg) was treated with different concentrations of each complex (50–250 μM) in the absence and presence of ascorbic acid, H_2Asc (100 μM). The total

volume of all samples was adjusted to 10 μL by adding HEPES buffer (40 mM HEPES, 10 mM $MgCl_2$). The reaction mixtures were incubated at 37 °C for 2 h, then a loading buffer (2 μL) consisting of 0.25% bromophenol blue, 0.25% xylene cyanol, and 30% glycerol was added. The samples were electrophoresed on 0.8% agarose gel in 1X TAE-buffer (40 mM Tris–acetate and 1 mM EDTA) at 50 V for 45 min. The gel was stained with EB solution for 5 min and then photographed under UV light. The proportion of each DNA form was estimated by the volume of the visualized DNA bands (volume = intensity × area) and calculated by the following equation;

$$\%\text{DNA Form I} = (\text{Volume of DNA Form I} \times 100)/(\text{Total volume of all DNA Forms}) \quad (3)$$

Mechanistic studies of the DNA cleavage process were carried out in the presence of H_2O_2 (50 μM), and typical ROS scavengers DMSO (150 μM), KI (50 μM), glycerol (100 μM), MeOH (150 μM), and *t*-BuOH (150 μM) were used as hydroxyl radical ($OH^{\cdot}$) scavengers and NaN_3 (100 μM) was used as a singlet oxygen ($^1O_2$) scavenger. These scavengers were added to plasmid pBR322 DNA (0.1 μg) prior to addition of the complexes (250 μM). All samples were prepared in HEPES buffer and incubated at 37 °C for 2 h and then analyzed according to the procedure described above.

Atomic force microscopy (AFM)

Plasmid pBR322 DNA (0.2 μg) was heated at 60 °C for 15 min to obtain the open circular form and then incubated with the complexes (50 and 100 μM for $[Cu(L)Cl_2]$ and 50 and 150 μM for $[Cu(L)ClO_4]ClO_4$) in the absence and presence of H_2Asc (100 μM) in 20 μL HEPES buffer at 37 °C for 2 h. Milli-Q water and all solutions for the AFM studies were filtered through 0.2 μM FP030/3 filters (Scheicher and Schuell GMbH, Germany) to obtain clear AFM images. After incubation, a drop (8 μL) of each sample was placed onto peeled mica disks (PELCO Mica Discs, 9.9 nm diameter; Ted Pella, Inc. California, USA) and allowed to absorb for 2 min at room temperature. The samples were rinsed for 5 s with a stream of Milli-Q water directed onto the surface and subsequently blown dry with argon before imaging.

Anticancer activity assay

Cancer cell growth inhibition tests were carried out against three cell lines, namely KB (epidermoid carcinoma of oral cavity, ATCC CCL-17), MCF-7 (breast adenocarcinoma, ATCC HTB-22) and NCI-H187 (small cell lung carcinoma, ATCC CRL-5804), using the resazurin microplate assay (REMA) [21]. Ellipticine, doxorubicin, and tamoxifen were used as positive controls, and 0.5% DMSO was used as a negative control. To investigate the potential cytotoxic behaviors of the complexes, cells in logarithmic growth phase were harvested and diluted in fresh medium to 7×10^4 cell mL^{-1} for KB, and 9×10^4 cell mL^{-1} for MCF-7 and NCI-H187. Subsequently, 5 μL of each test sample was diluted in 5% DMSO, and 45 μL aliquots of cell suspension were added to 384-well plates and then incubated at 37 °C in 5% CO_2. After the incubation period (3 days for KB and MCF-7, and 5 days for NCI-H187), 12.5 μL of 62.5 μg mL^{-1} resazurin solution was added to each well, and the plates were then incubated at 37 °C for 4 h. The fluorescence signal was measured using a SpectraMax M5 multi-detection microplate reader (Molecular Devices, USA) at excitation and emission wavelengths of 530 and 590 nm, respectively. The inhibition of cell growth was calculated with Eq. (4);

$$\%\text{Inhibition} = [1 \times (FU_T/FU_C)] \times 100 \quad (4)$$

where FU_T and FU_C are the mean fluorescence units from, respectively, treated and untreated with cells. The anticancer activities of the complexes are expressed as the 50% inhibitory concentration (IC_{50}), as determined from the dose–response curves using the SOFTMax Pro software (Molecular Devices, USA). The plotted data were obtained from six different concentrations of twofold serially diluted test samples. Results with $IC_{50} > 50$ μg mL^{-1} were considered as inactive [22].

Results and discussion

DNA-binding studies

Electronic absorption spectroscopy is widely employed to determine the binding affinities of metal complexes with DNA. Increasing absorbance or *hyperchromicity* results from base unstacking. Complexes which bind to DNA through intercalation usually manifest *hypochromism* (decrease in absorbance) and redshift (*bathochromism*) due to strong stacking interactions between the complex and the DNA base pairs [23]. A classical intercalator like ethidium bromide shows hypochromism as [24].

Absorption spectra of $[Cu(L)Cl_2]$ and $[Cu(L)ClO_4]ClO_4$ in the absence and presence of CT-DNA are shown in Fig. 2. The spectra of the pure complexes exhibit the same absorption pattern with two intense bands; one at 261 nm attributed to ligand-to-metal charge transfer (LMCT), and another at 201 nm attributed to an $n \rightarrow \pi^*$ or $\pi \rightarrow \pi^*$ transition of the ligands. Upon the addition of CT-DNA, the absorption bands of both complexes are affected, resulting in a clear hyperchromic effect and slight blueshift

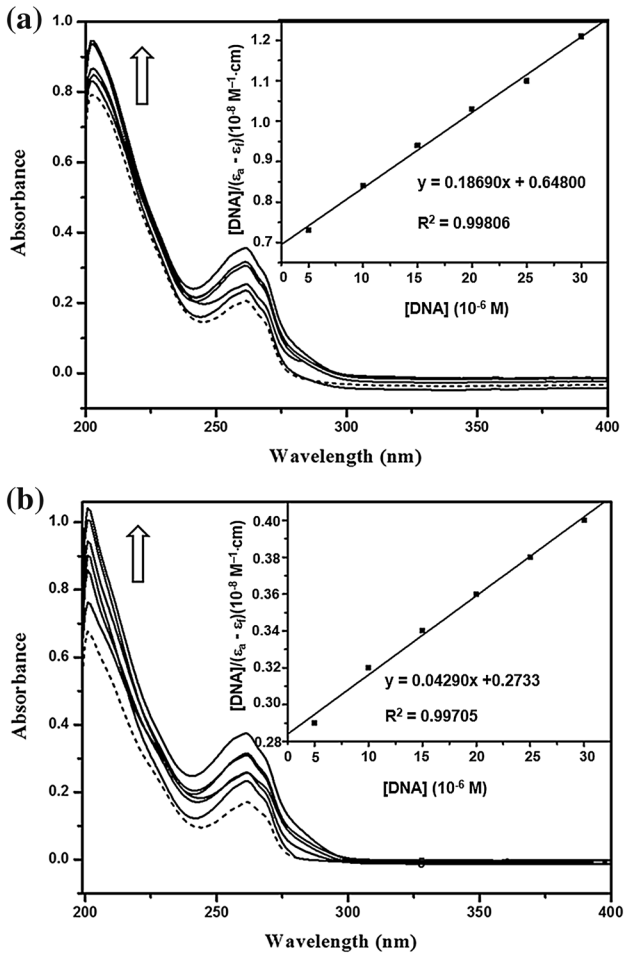

Fig. 2 Absorption spectra of $[Cu(L)Cl_2]$ (**a**) and $[Cu(L)ClO_4]ClO_4$ (**b**) in the absence (*dashed lines*) and presence (*line*) of CT-DNA from 0 to 30 μM. [Complex] = 50 μM. *Arrows* show the absorbance changes upon increasing DNA concentration

from 201 to 203 nm. Both complexes show similar hyperchromic effects, suggesting that they are likely to undergo a non-intercalative interaction with DNA.

The intrinsic binding constants (K_b) for both complexes were calculated using Eq. (1). The selected maximum absorbance at $\lambda_{max} = 201$ nm (A_{201}) for both complexes were used to calculate the K_b values, resulting in $2.81 \times 10^5\ M^{-1}$ for $[Cu(L)Cl_2]$ and $1.57 \times 10^5\ M^{-1}$ for $[Cu(L)ClO_4]ClO_4$. These values are lower than that of the classical intercalator ethidium bromide ($1.0 \times 10^7\ M^{-1}$) [25], but higher than those of other complexes with the CuN_3X_2 chromophore [26–30] (Table 1). The similar K_b values for both complexes indicate similar DNA-binding behaviors, consistent with their nucleobase-binding properties in the previous report [14].

Fluorescence spectroscopy is often used to investigate the competitive interactions between metal complexes and the classical DNA intercalator ethidium bromide. Free EB is only weakly fluorescent, but in the presence of DNA, its fluorescence is markedly increased, with an emission band at about 600 nm, resulting from intercalation of EB between adjacent DNA base pairs. This fluorescence can be competitively quenched by the addition of a second molecule [31].

Emission spectra of EB bound to DNA in the absence and presence of the present complexes are shown in Fig. 3. For both complex, their interaction into the EB-DNA solution resulted in decrease in the emission intensity of EB, indicating the displacement of EB by the complexes. The binding strength of each complex with CT-DNA was calculated as the linear Stern–Volmer quenching constant (K_{sv}). From the plot of F_0/F versus [Complex] (Fig. 3), the calculated K_{sv} values were obtained from the slopes as 2.00×10^3 and $1.83 \times 10^3\ M^{-1}$ for $[Cu(L)Cl_2]$ and $[Cu(L)ClO_4]ClO_4$, respectively.

Although the K_b and K_{sv} values of both complexes are different, they have the same trend. The K_b values apply to the binding capabilities of the complexes toward free double stranded DNA while the K_{sv} values are a measure of their competitive binding to the EB-bound DNA.

To further clarify the nature of the interaction between the complexes and DNA, viscosity measurements were carried out on CT-DNA solutions with various concentrations of the complexes. A classical intercalator such as EB is expected to increase the separation of the base pairs, giving an increase in overall DNA length and consequently an increase in the DNA viscosity (Fig. 4). In contrast, partial and/or non-classical intercalation of the complexes can bend (or kink) the DNA helix, reducing its effective length and viscosity [32].

The effects of these complexes on the viscosity of CT-DNA are shown in Fig. 4, which reveals that the relative viscosity of CT-DNA in the presence of the complexes depends upon the complex concentration. There are three effects consisting of a reduction, enhancement and steadiness in viscosity. In the first effect, a dramatic reduction in viscosity was found for [Complex]/[DNA] ratios of 0.0–0.5 for both complexes. This outcome is opposite to the case of EB which raises the DNA viscosity. Consequently, the two complexes possibly bind to DNA through non-intercalative interactions. On the other hand, the second effect was a marked increase in viscosity, in the narrow r range of 0.5–0.8 for both complexes, thus indicating that intercalative binding of the complexes may occur in this concentration range. Finally, when raising the r ratio higher than 0.8, no further change in viscosity was observed. It is possible that the interactions may be electrostatic or groove binding [33] or that the binding sites may reach the saturation point at higher concentrations of the complexes. The similar behaviors of both complexes imply that they exhibit the same binding behaviors.

Table 1 Comparison of the DNA-binding ability between the two CuN_3X_2 complexes in this work and the previous works

Compound	Proposed binding modes	K_b (M^{-1})	References
$[Cu(L)Cl_2]$	Non-intercalation	2.81×10^5	This work
$[Cu(L)ClO_4]ClO_4$	Non-intercalation	1.57×10^5	This work
Ethidium bromide (EB)	Intercalation	1.00×10^7	[25]
$[Cu(BMA)Cl_2](CH_3OH)$[a]	Intercalation	1.24×10^4	[26]
$[Cu(L^1)Cl_2]$[b]	Non-intercalation	2.00×10^4	[27]
$[Cu(L^2)(H_2O)_2](NO_3)_2$[c]	Non-intercalation	8.00×10^4	[28]
$[Cu(Pyimpy)(Cl)(ClO_4)]$[d]	Covalent bond	5.20×10^3	[29]
$[Cu(Pyimpy)Cl_2](H_2O)_2$[d]	Covalent bond	4.00×10^3	[30]

[a] BMA = *N*,*Ń*-bis(benzimidazol-2-yl-ethyl)amine

[b] L^1 = bis(2-benzimidazolylmethyl)amine

[c] L^2 = 2,6-bis-(benzimidazolyl)pyridine

[d] Pyimpy = 2-((2-phenyl-2-(pyridin-2-l)hydazono)methyl)pyridine

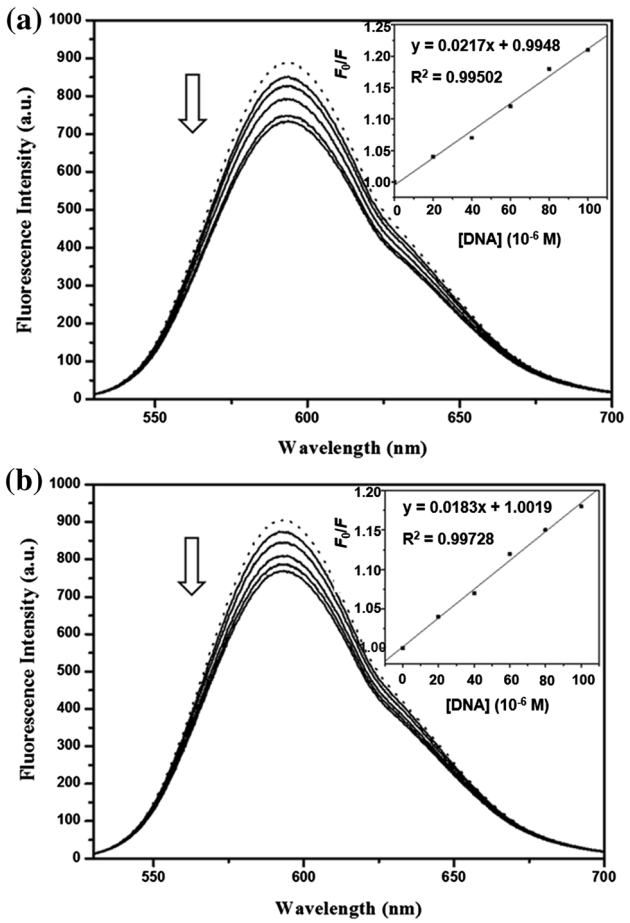

Fig. 3 Emission spectra of EB (100 μM) bound to DNA (100 μM) in the absence (*dotted lines*) and presence (*line*) of complexes (20, 40, 60, 80 and 100 μM); $[Cu(L)Cl_2]$ (**a**) and $[Cu(L)ClO_4]ClO_4$ (**b**). *Arrows* show the absorbance changes upon increasing complexes concentration

Circular dichroism spectroscopy is a useful technique to assess whether nucleic acids undergo conformational changes as a result of complex-DNA formation. The CD

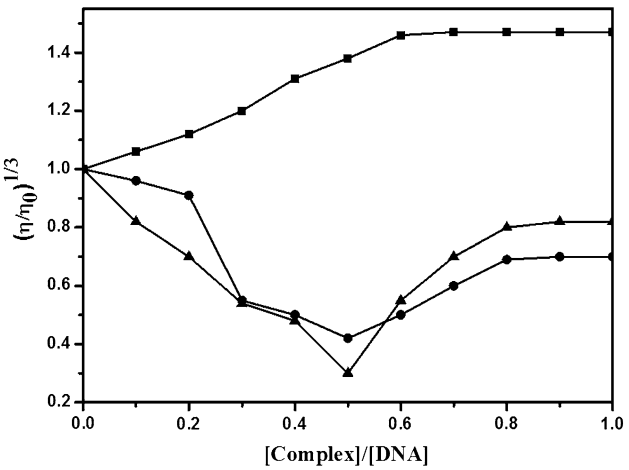

Fig. 4 Effect of increasing amounts of EB (*solid square*), $[Cu(L)Cl_2]$ (*solid triangle*) and $[Cu(L)ClO_4]ClO_4$ (*solid round*) on the relative viscosity of CT-DNA vs. the [Complex]/[DNA] ratio at 37 ± 0.1 °C, [DNA] = 100 μM

spectrum of CT-DNA consists of a positive band at 277 nm due to base stacking and a negative band at 245 nm because of helicity, which is a characteristic of the right-handed B form of DNA [34]. Changes in the CD spectrum of DNA upon the complexes may often be assigned to corresponding changes in DNA structure [35]. In general, non-intercalative interactions of small molecules with DNA show little or no perturbation on the base stacking and helicity bands of the CD spectrum because these binding modes do not significantly influence the secondary structure of DNA. On the other hand, a classical intercalator tends to enhance the intensities of both bands due to strong base stacking interactions and stable DNA conformations (right-handed B conformation of DNA).

CD spectra of CT-DNA in the absence and presence of the complexes are shown in Fig. 5. For both complexes, slight decreases in intensity of both the positive DNA band

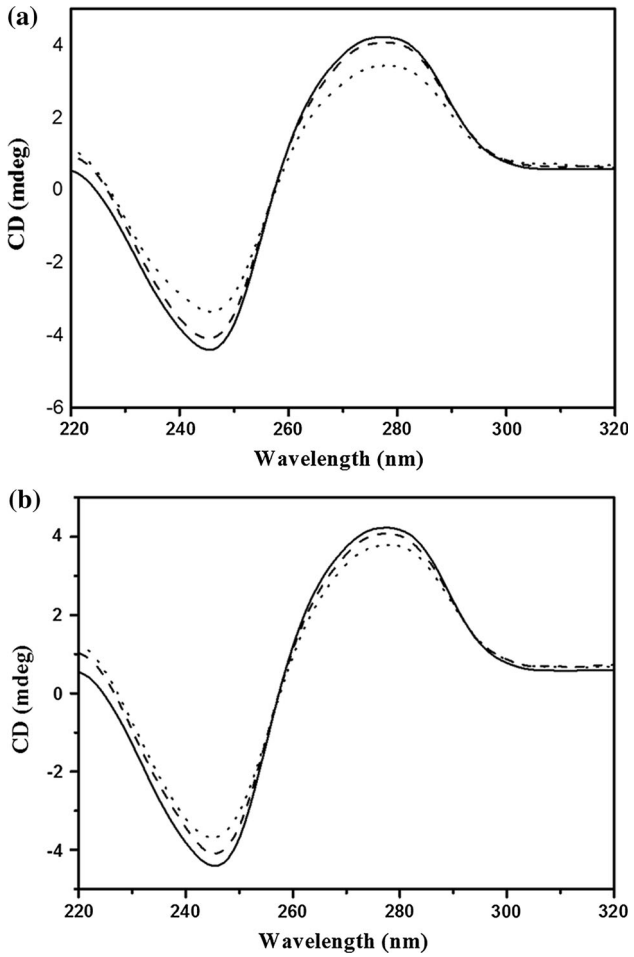

Fig. 5 Circular dichroism spectra of CT-DNA (70 μM) in the absence (*line*) and presence of $[Cu(L)Cl_2]$ (**a**) and $[Cu(L)ClO_4]ClO_4$ (**b**) at the [Complex]/[DNA] ratio of 0.5 (*dashed lines*) and 1.0 (*dotted lines*)

at 277 nm and negative band at 245 nm were observed with increasing [Complex]/[DNA] ratios. These observations are similar to the effect of the copper(II) complexes of bis(pyrid-2-yl)-di/trithia ligands [36] and 2,9-dimethyl-1,10-phenanthrolines [37]. It suggests that electrostatic and/or groove binding may constitute the major interaction between DNA and these complexes.

DNA-melting analysis and stoichiometry

To better understand the function of these complexes when interacting with DNA in terms of stabilization or destabilization of DNA strands, thermal denaturation experiments were carried out. In such experiments, the stabilizing forces of the DNA double helix are overcome by melting or denaturation. A higher or lower T_m value of the complex-bound DNA compared to free DNA suggests that the complexes stabilize or destabilize the DNA strands, respectively. Hence, the melting temperature difference (ΔT_m) can suggest the possible interaction type between complexes and DNA. Intercalation of natural or synthetic organics and metallointercalators generally results in a considerable increase in melting temperature and high ΔT_m value. Neyhart et al. and Kumar et al. [38, 39] showed that the intercalation into DNA can increase the stability of the helix, resulting in ΔT_m values of 5–14 °C. Low ΔT_m values (close to zero) are indicative of non-intercalative binding modes [40, 41]. Moreover, negative ΔT_m values suggest that groove and/or electrostatic interactions may be the primary binding modes [41].

The T_m values of CT-DNA at different [Complex]/[DNA] ratios ($r = 0.1$, 0.2, 0.3 and 0.4) are presented in Fig. A1 and Table 2. The T_m value of CT-DNA (100 μM) was measured as 81.0 °C. The T_m values gradually decreased for r ratios increasing from 0.1 to 0.4. Both complexes stabilize DNA at $r = 0.1$ and 0.2, but destabilize DNA at $r = 0.3$ and 0.4. Furthermore, the low ΔT_m values (close to zero) of both complexes indicate that a non-intercalative mode is likely to be the main interaction in this system. Specifically, the two complexes at $r = 0.3$ and 0.4 may bind to DNA by groove binding and/or electrostatic interactions due to the negative ΔT_m values [41].

Determination of the DNA-binding stoichiometry of the complexes, expressed as Cu (mmol)/DNA (mol base), is an additional method to obtain information regarding these interactions. The stoichiometric ratio can be determined from atomic absorption and UV–Vis spectroscopic measurements. We found that $[Cu(L)Cl_2]$ and $[Cu(L)ClO_4]$-ClO_4 gave Cu (mmol)/DNA (mol base) ratios of 26 and 12, respectively. These values can be compared with the Cu (mmol)/DNA (mol base) ratios of known copper(II) compounds. For example, $[Cu(H_2O)_6]^{2+}$ with the ratio > 150 shows poorly selective DNA binding, most likely due to the interaction of this cationic species with the negatively charged phosphate groups on the DNA backbone, while a Cu(II)-dipeptide gave a ratio < 42, suggesting a more efficient DNA interaction [20]. The two copper compounds in the present work shows similar values to the latter, suggesting similar DNA-binding affinity.

DNA cleavage studies

The nuclease activities of the complexes were studied by gel electrophoresis using plasmid pBR322 DNA in the absence and presence of ascorbic acid (H_2Asc) as a reducing agent. In general, when plasmid DNA is subjected to electrophoresis, the fastest migration will be observed for the supercoiled form (Form I). If scission occurs on one strand, the supercoil will relax to generate a slower-moving nicked circular form (Form II). If both strands are cleaved, a linear form (Form III) that migrates between Forms I and II will be obtained.

Table 2 Thermal melting temperature (T_m) and the melting temperature difference ($\Delta T_m = T_{m\ (of\ bound\ to\ DNA)} - T_{m\ (of\ the\ free\ DNA)}$) in the presence of the $[Cu(L)Cl_2]$ and $[Cu(L)ClO_4]ClO_4$ complexes

r	T_m		ΔT_m	
	$[Cu(L)Cl_2]$	$[Cu(L)ClO_4]ClO_4$	$[Cu(L)Cl_2]$	$[Cu(L)ClO_4]ClO_4$
0.1	82.0	82.6	+1.0	+1.6
0.2	81.7	81.5	+0.7	+0.5
0.3	80.7	80.1	−0.3	−0.9
0.4	78.7	79.0	−1.3	−2.0

The melting point of the free CT-DNA is 81.0 °C

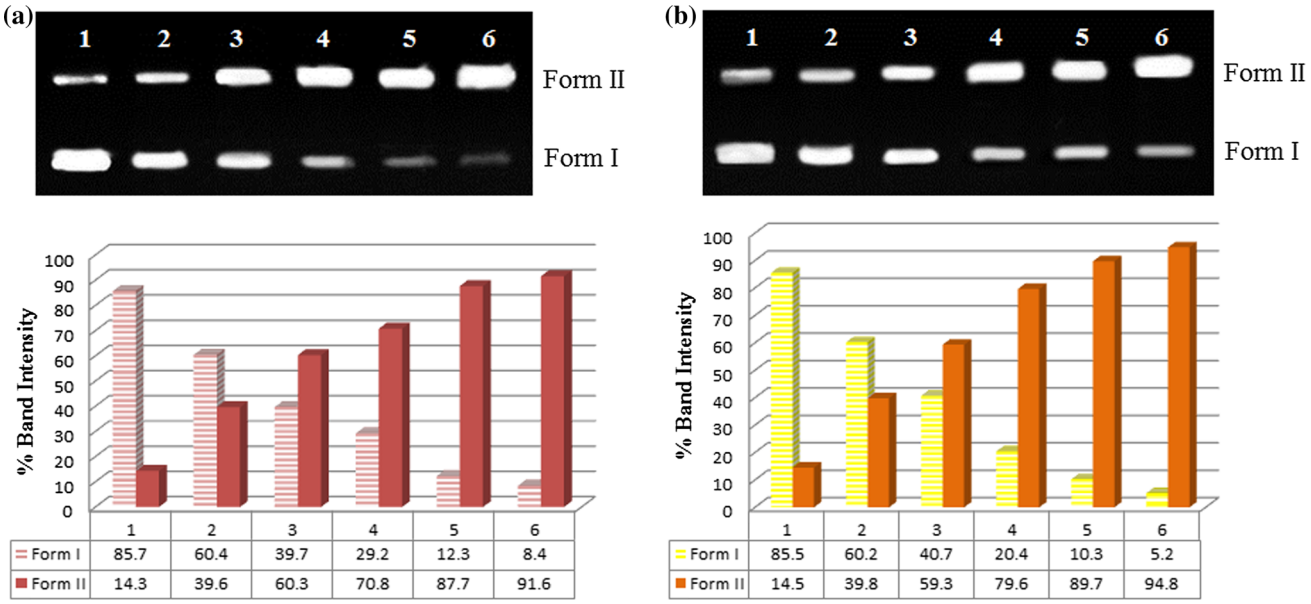

Fig. 6 Electrophoretic diagrams showing the cleavage of supercoiled pBR322 DNA (0.1 μg) by $[Cu(L)Cl_2]$ (**a**) and $[Cu(L)ClO_4]ClO_4$ (**b**) in HEPES buffer at 37 °C for 2 h with histogram of % band intensity of DNA: Lane 1, DNA control; *Lanes 2–6*, DNA + [complex] (50, 100, 150, 200 and 250 μM, respectively)

The results of gel electrophoretic separation of pBR322 DNA after incubation 2 h with the copper(II) complexes in the absence and presence of H_2Asc are shown in Figs. 6, 7, respectively. In the absence of H_2Asc, $[Cu(L)Cl_2]$ (Fig. 6a) and $[Cu(L)ClO_4]ClO_4$ (Fig. 6b) are able to bring about conversion of Form I to Form II. The amount of Form II was found to increase with increasing complex concentration, from 50 to 250 μM. However, the formation of Form III was not observed under these conditions.

It is known that the DNA-cleaving potential of transition metal complexes can be enhanced by adding exogenous redox reagents such as hydrogen peroxide and ascorbic acid. Herein, H_2Asc was used to mimic the reducing environment, found inside the cells, and will induce the formation of copper(I) species from the present complexes. Under an aerobic atmosphere, this would allow the formation of reactive oxygen species (ROS) that are able to cleave DNA. In the presence of H_2Asc, the nuclease activities of both complexes were dramatically improved (Fig. 7). Upon increasing the complex concentration (Lanes 4–8 in Fig. 7), Form I plasmid DNA was converted into Form II and then Form III, initially observed at 100 μM for $[Cu(L)Cl_2]$ and 150 μM for $[Cu(L)ClO_4]ClO_4$. At a complex concentration of 250 μM in the presence of H_2Asc (Lane 8), $[Cu(L)Cl_2]$ gives exclusively DNA Form III (100%), while $[Cu(L)ClO_4]ClO_4$ gives a mixture of Form II (17.3%) and Form III (82.7%). These results follow the same trend as the DNA-binding abilities of the complexes.

Such behavior leads us to assume that DNA cleavage by both complexes in the presence of H_2Asc is most likely to involve ROS such as hydroxyl radical, singlet oxygen or superoxide, all of which can cleave DNA [42]. The role of these copper(II) complexes can be related to the enzymatic

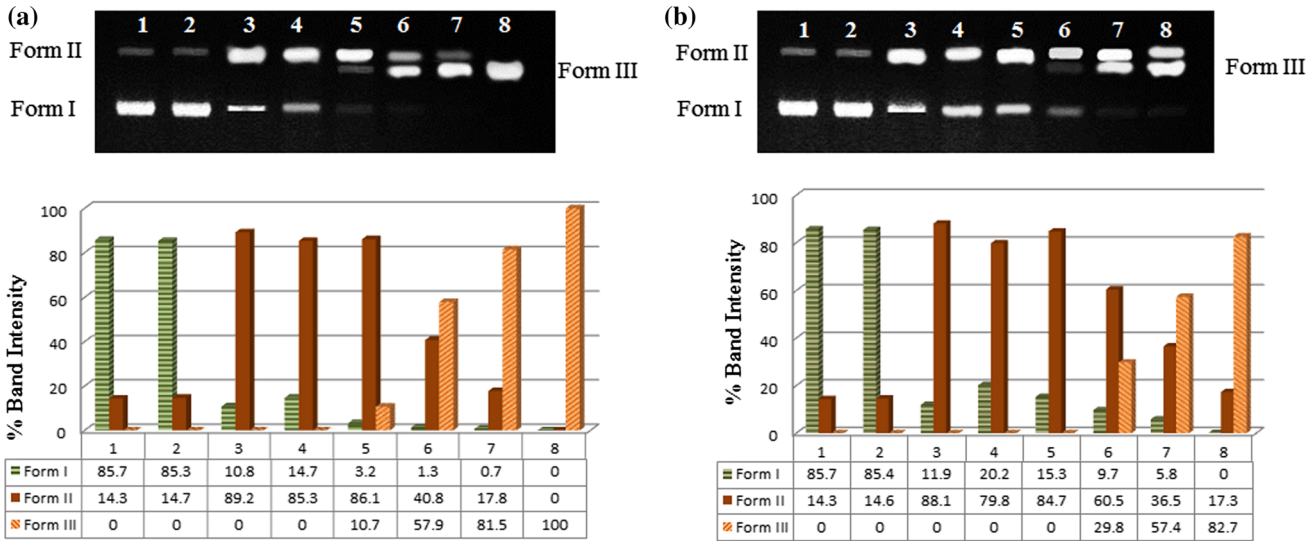

Fig. 7 Electrophoretic diagrams showing the cleavage of supercoiled pBR322 DNA (0.1 μg) by $[Cu(L)Cl_2]$ (**a**) and $[Cu(L)ClO_4]ClO_4$ (**b**), in the presence of H_2Asc (100 μM) in HEPES buffer at 37 °C for 2 h with histogram of % band intensity of DNA: *Lane 1*, DNA control; *Lane 2*, DNA + H_2Asc; *Lane 3*, DNA + complex (250 μM); *Lanes 4–8*, DNA + H_2Asc + [complex] (50, 100, 150, 200 and 250 μM, respectively)

properties of copper, which are important to the proposed mechanism for in situ formation of H_2O_2 as shown below [43].

$$H_2Asc + H_2O \rightleftharpoons HAsc^- + H_3O^+ \quad (5)$$

$$HAsc^- + 2Cu(II) \rightarrow Asc + 2Cu(I) + H^+ \quad (6)$$

$$2Cu(I) + O_2 + 2H^+ \rightarrow 2Cu(II) + H_2O_2 \quad (7)$$

$$HAsc^- + O_2 + H^+ \rightarrow Asc + H_2O_2 \quad (8)$$

As shown in reactions (5)–(8), Cu(II) will be reduced by ascorbate to Cu(I), which reacts with dioxygen under aerobic conditions to yield H_2O_2. The overall reaction corresponds to the autooxidation of ascorbate ion, which may involve a single two-electron oxidation step [44]. Finally, hydrogen peroxide reacts with another equivalent of Cu(I) through the Fenton reaction (9) producing hydroxyl radical, responsible for DNA oxidative damage [43].

$$Cu(I) + H_2O_2 \rightarrow Cu(II) + OH^- + OH^{\cdot} \quad (9)$$

To confirm the proposed DNA cleavage mechanism described above, exogenous hydrogen peroxide was added to the DNA–copper(II) complex system to directly produce ROS. In certain reports [45], if DNA cleavage occurs via a hydrolytic pathway, the nuclease activity will not involve hydroxyl radical, singlet oxygen or superoxide. On the other hand, the nuclease activity will depend on ROS, if it proceeds via an oxidative pathway. We therefore investigated the possible cleavage mechanism by using ROS scavengers, specifically DMSO, KI, glycerol, MeOH and *t*-BuOH as hydroxyl radical scavengers and NaN_3 as a singlet oxygen scavenger.

The cleavage of supercoiled pBR322 DNA (Form I) in the presence of the scavengers alone was studied by gel electrophoresis, as shown in Fig. A2. The results show that hydroxyl radical and singlet oxygen scavengers do not damage the DNA (Lanes 2 – 7). KI causes the slow migration of DNA (Lane 3), possibly arising from a DNA-KI adduct [46]. Figure 8 shows the cleavage of pBR322 DNA by the complexes in the presence of scavengers after incubation at 37 °C for 2 h. DNA is not affected by hydrogen peroxide alone (Lane 2). On incubation of either complex with pBR322 DNA in the presence of H_2O_2 (Lane 4), the amount of Form II obtained was considerably greater than in the presence of the complexes alone (Lane 3). This indicates that hydrogen peroxide actively assists the copper(II) complexes in DNA degradation by oxidative cleavage. In the presence of hydroxyl radical scavengers (Lanes 5–9), inhibition of DNA conversion from Form I to Form II was observed. On the other hand, the presence of NaN_3 as a singlet oxygen quencher (Lane 10) showed no significant effect on the DNA cleavage. Hence, the hydroxyl radical is most likely to be the ROS responsible for oxidative DNA cleavage.

AFM analysis

To further confirm the effect of the complexes on the DNA structure, atomic force microscopy (AFM) was carried out with pBR322 plasmid DNA. After incubation, the changes in DNA morphology caused by the complexes were visualized by AFM, as shown in Fig. 9. The supercoiled DNA alone (Form I) (Fig. 9a) is not affected by H_2Asc (Fig. 9b).

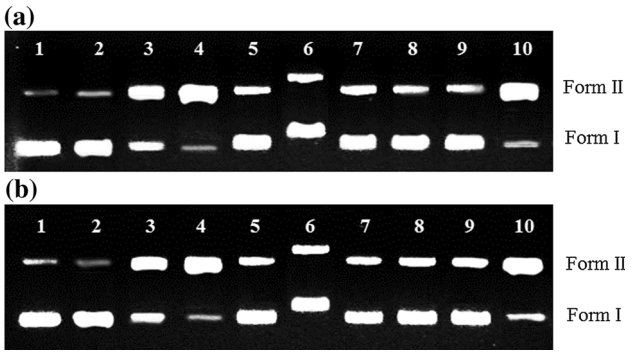

Fig. 8 Electrophoretic diagrams showing the cleavage of supercoiled pBR322 DNA (0.1 μg) by $[Cu(L)Cl_2]$ (**a**) and $[Cu(L)ClO_4]ClO_4$ (**b**) (250 μM) in the presence of H_2O_2 (50 μM) in HEPES buffer at 37 °C with an incubation time of 2 h: *Lane 1*, DNA control; *Lane 2*, DNA + H_2O_2; *Lane 3*, DNA + complex; *Lanes 4*, DNA + complex + H_2O_2; *Lanes 5–10*, DNA + complex + H_2O_2 + scavenger (DMSO (150 μM), KI (50 μM), glycerol (100 μM), MeOH (150 μM), *t*-BuOH (150 μM) and NaN_3 (100 μM), respectively)

In contrast, both complexes induce significant alterations in the DNA morphology; in fact, the complexes can cleave the biomolecule to Form II and Form III (Fig. 9c–f), corroborating the data from electrophoresis (see Lanes 4 and 5 in Fig. 7a for $[Cu(L)Cl_2]$; Lanes 4 and 6 in Fig. 7b for $[Cu(L)ClO_4]ClO_4$). Therefore, both complexes can act as efficient DNA-cleaving agents.

Table 3 Cancer cell growth inhibition of $[Cu(L)Cl_2]$ and $[Cu(L)ClO_4]ClO_4$ and cisplatin

Complex	IC_{50} (μg mL^{-1})		
	MCF-7	NCI-H187	KB
$[Cu(L)Cl_2]$	Inactive	3.35	7.65
$[Cu(L)ClO_4]ClO_4$	Inactive	4.83	13.05
Cisplatin	Inactive	Inactive	27.01

Cytotoxicity assays

Since both of these complexes show DNA-binding and cleaving capabilities, their anticancer activity was further investigated against three human cell lines (MCF-7, NCI-H187 and KB) and compared with the first generation anticancer drug cisplatin. Results are expressed as the IC_{50} value, as shown in Table 3. Both copper(II) complexes show cytotoxicity against NCI-H187 and KB cell lines, but

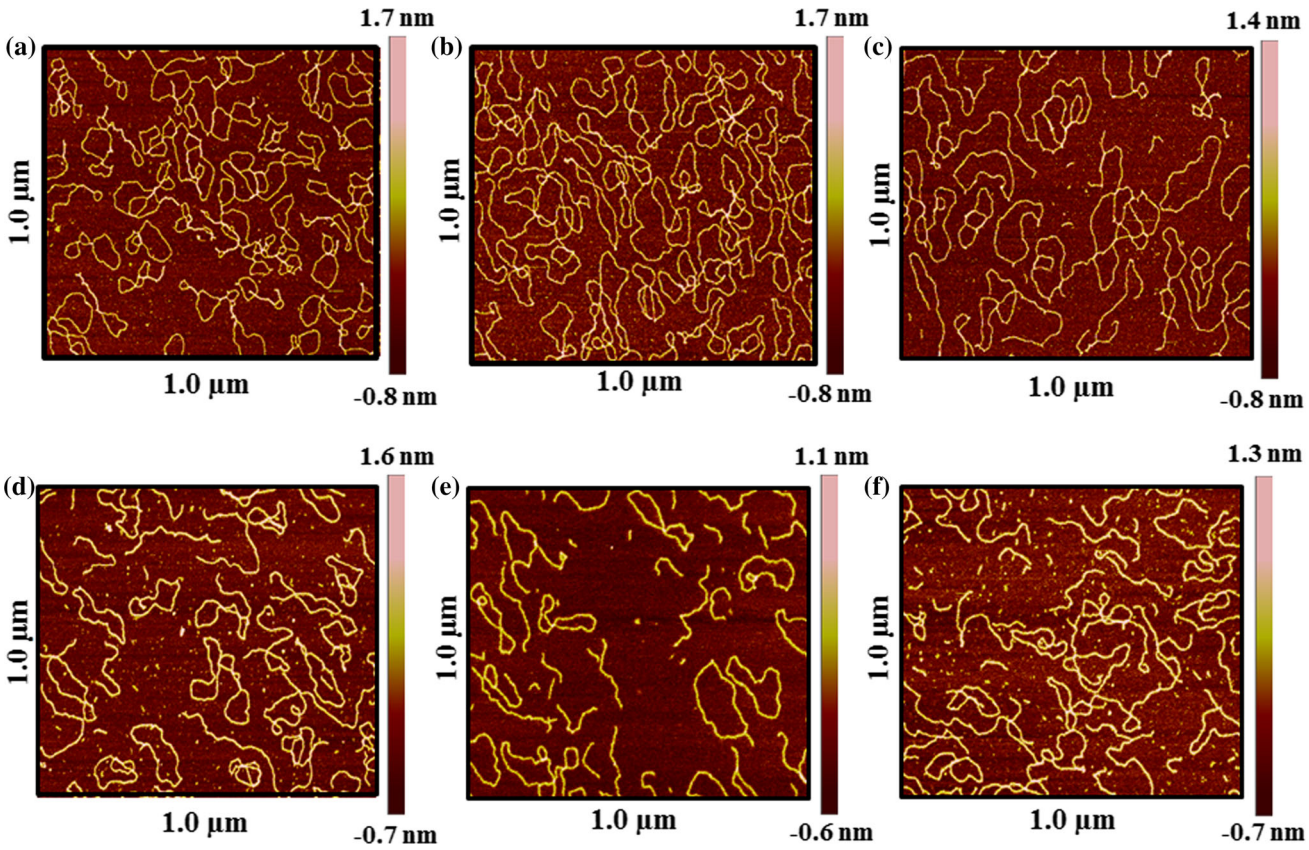

Fig. 9 AFM images of plasmid pBR322 DNA (0.2 μg) in the presence of H_2Asc (100 μM) with various concentration of the complexes. Pure plasmid DNA (**a**); DNA + H_2Asc (**b**); DNA + H_2Asc + $[Cu(L)Cl_2]$ (50 μM) (**c**); DNA + H_2Asc + $[Cu(L)ClO_4]ClO_4$ (50 μM) (**d**); DNA + H_2Asc + $[Cu(L)Cl_2]$ (100 μM) (**e**); DNA + H_2Asc + $[Cu(L)ClO_4]ClO_4$ (150 μM) (**f**), with incubation time of 2 h at 37 °C in HEPES buffer, pH 7.1

are inactive against the MCF-7 cell line. Interestingly, both complexes are more active than cisplatin under these experimental conditions, giving the best activity toward NCI-H187.

Conclusion

Two copper(II) complexes of *N*-(methylpyridin-2-yl)-amidino-*O*-methylurea containing different anionic co-ligands have been investigated for biological potential. Their DNA-binding abilities occur through non-intercalative modes. They also show chemical nuclease properties via oxidative DNA cleavage. Furthermore, the anticancer activities of both complexes appear to be superior to that of cisplatin. These results indicate that the DNA-interacting properties and cytotoxicities of such complexes are related. This may come from the fact that they contain the same cationic species in solution phase, $[Cu(L)(H_2O)_x]^{2+}$ ($x = 1$–3), thus revealing similar properties to our previous work [14]. We conclude that such complexes have potential as DNA-damaging agents for use in cancer therapy.

Acknowledgements This work was financially supported by Center of Excellence for Innovation in Chemistry (PERCH-CIC) and the Higher Education Research Promotion and National Research University Project of Thailand, Office of the Higher Education Communication, through the Advanced Functional Materials Cluster of Khon Kaen University. P.G. acknowledges ICREA (Institució Catalana de Recerca i Estudis Avançats), the Ministerio de Economía y Competitividad of Spain (Project CTQ2011-27929-C02-01), and the support of COST Actions CM1003 and CM1105.

References

1. Shahabadi N, Kashanian S, Darabi F (2010) DNA binding and DNA cleavage studies of a water soluble cobalt(II) complex containing dinitrogen Schiff base ligand: the effect of metal on the mode of binding. Eur J Med Chem 45:4239–4245
2. Parveen S, Arjmand F, Ahmad I (2014) Enantiomeric in vitro DNA binding, pBR322 DNA cleavage and molecular docking studies of chiral L- and D-ternary copper(II) complexes of histidine and picolinic acid. J Photochem Photobiol, B 130:170–178
3. Pradeepa SM, Naik HSB, Kumar BV, Priyadarsini KI, Barik A, Jayakumar S (2015) Synthesis and characterization of cobalt(II), nickel(II) and copper(II)-based potential photosensitizers: evaluation of their DNA binding profile, cleavage and photocytotoxicity. Inorg Chim Acta 428:138–146
4. Arjmand F, Jamsheera A, Mohapatra DK (2013) Synthesis, characterization and in vitro DNA binding and cleavage studies of Cu(II)/Zn(II) dipeptide complexes. J Photochem Photobiol, B 121:75–85
5. Sangeetha S, Murali M (2015) Water soluble copper(II) complex $[Cu(dipica)(CH_3COO)]ClO_4$: dNA binding, pH dependent DNA cleavage and cytotoxicity. Inorg Chem Commun 59:46–49
6. Kumar RS, Sasikala K, Arunachalam S (2008) DNA interaction of some polymer–copper(II) complexes containing 2,2′-bipyridyl ligand and their antimicrobial activities. J Inorg Biochem 102:234–241
7. Chaveerach U, Meenongwa A, Trongpanich Y, Soikum C, Chaveerach P (2010) DNA binding and cleavage behaviors of copper(II) complexes with amidino-*O*-methylurea and *N*-methylphenyl-amidino-*O*-methylurea, and their antibacterial activities. Polyhedron 29:731–738
8. Meenongwa A, Brissos RF, Soukum C, Chaveerach P, Gamez P, Trongpanich Y, Chaveerach U (2015) DNA-interacting and biological properties of copper(II) complexes from amidino-*O*-methylurea. New J Chem 39:664–675
9. Qiu L, Lv G, Guo L, Chen L, Luo S, Zou M, Lin J (2015) Synthesis, crystal structure and antitumor effect of a novel copper(II) complex bearing zoledronic acid derivative. Eur J Med Chem 89:42–50
10. Meenongwa A, Chaveerach U, Blake AJ (2012) Methanol[1-(methoxy methanimidoyl)-2-(pyridin-2-ylmethyl)guanidine]bis(perchlorato)copper(II). Acta Crystallogr Sect C 68:m143–m146
11. Hubberstey P, Suksangpanya U (2004) Hydrogen-bonded supramolecular chain and sheet formation by coordinated guanidine derivatives. Struct Bond 111:33–83
12. Sączewski F, Balewski Ł (2013) Biological activities of guanidine compounds, 2008–2012 update. Expert Opin Ther Pat 23:965–995
13. Roa AVR, Gurjar MK, Islam A (1993) Synthesis of a new bicyclic guanidine heterocycle as a potential anti HIV agent. Tetrahedron Lett 34:4993–4996
14. Pratumwieng R, Soikum C, Chaveerach P, Chaveerach U (2014) Binding studies of (*N*-(methylpyridin-2-yl)-amidino-*O*-methylurea)copper(II) complexes to four nitrogenous bases and 5′-GMP. Inorg Chim Acta 423:421–429
15. Suksangpanya U, Blake AJ, Cade EL, Hubberstey P, Parker DJ, Wilson C (2004) Hydrogen-bonded supramolecular architectures in (*N*-(methylpyridin-2-yl)-amidino-*O*-alkylurea)copper(II) halides. CrystEngComm 6:159–167
16. Marmur J (1961) A procedure for the isolation of deoxyribonucleic acid from microorganisms. J Mol Biol 3:208–218
17. Reichman ME, Rice SA, Thomas CA, Doty P (1954) A further examination of the molecular weight and size of desoxypentose nucleic acid. J Am Chem Soc 76:3047–3053
18. Wolf A, Shimer GH, Meehan T (1987) Polycyclic aromatic hydrocarbons physically intercalate into duplex regions of denatured DNA. Biochemistry 26:6392–6396
19. Lakowicz JR, Weber G (1973) Quenching of fluorescence by oxygen. A probe for structural fluctuations in macromolecule. Biochemistry 12:4161–4170
20. Facchin G, Kremer E, Barrio DA, Etcheverry SB, Costa-Filho AJ, Torre MH (2009) Interaction of Cu-dipeptide complexes with Calf Thymus DNA and antiproliferative activity of [Cu(ala-phe)] in osteosarcoma-derived cells. Polyhedron 28:2329–2334
21. Brien JO, Wilson I, Orton T, Pognan F (2000) Investigation of the Alamar blue (resazurin) floresecence dye for the assessment of mammalian cell cytotoxicity. Eur J Biochem 267:5421–5426
22. O′Neill MJ MJ, Bray DH, Boardmann P, Phillipson JD, Warhurst DC (1985) Plants as sources of antimalarial drugs part 1. *In vitro* test method for the evaluation of crude extracts from plants. Planta Med 51:394–398
23. Barton JK, Danishefsky A, Goldberg J (1984) Tris(phenanthroline) ruthenium(II): stereoselectivity in binding to DNA. J Am Chem Soc 106:2172–2176
24. Long EC, Barton JK (1990) On demonstrating DNA intercalation. Acc Chem Res 23:271–273
25. LePecq JB, Paoletti C (1967) A fluorescence complex between ethidium bromide and nucleic acids, Physical-chemical characterization. J Mol Biol 27:87–106

26. Qiao X, Ma ZY, Shao J, Bao WG, Xu JY, Qiang ZY, Lou JS (2014) Biological evaluation of a cytotoxic 2-substituted benzimidazole copper(II) complex: DNA damage, antiproliferation and apoptotic induction activity in human cervical cancer cells. Biometals 27:155–172
27. Chen Z, Wang X, Li Y, Guo Z (2008) Comparison of DNA binding and cleavage abilities between mono- and trinuclear copper(II) complexes of benzimidazole derivatives. Inorg Chem Commun 11:1392–1396
28. Dey S, Sarkar S, Paul H, Zangrando E, Chattopadhyay P (2010) Copper(II) complex with tridentate N donor ligand: synthesis, crystal structure, reactivity and DNA binding study. Polyhedron 29:1583–1587
29. Ghosh K, Kuma P, Tyagi N, Singh UP, Goel N (2011) Synthesis, structural characterization and DNA interaction studies on a mononuclear copper complex: nuclease activity via self-activation. Inorg Chem Commun 14:489–492
30. Ghosh K, Kumar P, Tyagi N, Singh UP, Goel N, Chakraborty A, Roy P, Baratto MC (2011) DNA interaction, superoxide scavenging and cytotoxicity studies on new copper(II) complexes derived from a tridentate ligand. Polyhedron 30:2667–2677
31. Baguley BC, Bret ML (1984) Quenching of DNA-ethidium fluorescence by amsacrine and other antitumor agents: a possible electron-transfer effect. Biochemistry 23:937–943
32. Scaria PV, Shafer RH (1991) Binding of ethidium bromide to a DNA triple helix. J Biol Chem 266:5417–5423
33. Kelly JM, Tossi AB, McConnell DJ, Ohuigin C (1985) A study of the interactions of some polypyridylruthenium(II) complexes with DNA using fluorescence spectroscopy, topoisomerisation and thermal denaturation. Nucleic Acids Res 14:6017–6034
34. Johnson WC (1994) In: Nakanishi K, Berova N, Woody RW (eds) Circular dichroism: Principle and application. VCH, New York
35. Lincoln P, Tuite E, Nordén B (1997) Short-circuiting the molecular wire: cooperative binding of Δ-[Ru(phen)2d ppz]2 + and Δ-[Ru(phi)2bipy]3 + to DNA. J Am Chem Soc 119:1454–1455
36. Mahadevan S, Palaniandavar M (1997) Spectroscopic and voltammetric studies of copper(II) complexes of bis(pyrid-2-yl)-di/trithia ligands bound to calf thymus DNA. Inorg Chim Acta 254:291–302
37. Mahadevan S, Palaniandavar M (1998) Spectroscopic and voltammetric studies on copper complexes of 2,9-dimethyl-1,10-phenanthrorines bound to calf thymus DNA. Inorg Chem 37:693–700
38. Neyhart GA, Grover N, Smith SR, Kalsbeck WA, Fairley TA, Cory M, Thorp HH (1993) Binding and kinetics studies of oxidation of DNA by oxoruthenium (IV). J Am Chem Soc 115:4423–4428
39. Kumar CV, Punzalan EHA, Tan WB (2000) Adenine-thymine base pair recognition by an anthryl probe from the DNA minor groove. Tetrahedron 56:7027–7040
40. Schilter D, Urathamakul T, Beck JL, Harding MM, Rendina LM (2010) ESI-MS and thermal melting studies of nanoscale platinum(II) metallomacrocycles with DNA. Dalton Trans 39:11263–11271
41. Eichhorn GL, Shin YA (1968) Interaction of metal ions with polynucleotides and related compounds. XII. The relative effect of various metal ions on DNA helicity. J Am Chem Soc 90:7323–7328
42. Halliwell B, Gutteridge JMC (1999) Free Radicals in Biology and Medicine. Oxford Science Publication, Oxford
43. Sigman DS, Chen CHB (1986) Nuclease activity of 1,10-phenanthroline-copper ion. Acc Chem Res 19:180–186
44. Yamazaki I, Piette LH (1961) Mechanism of free radical formation and disappearance during the ascorbic oxidase and peroxidase. Biochem Biophys Acta 59:62–69
45. Barve A, Kumbhar A, Bhat M, Joshi B, Butcher R, Sonawane U, Joshi R (2009) Mixed-ligand copper(II) maltolate complexes: synthesis, characterization, DNA binding and cleavage, and cytotoxicity. Inorg Chem 48:9120–9132
46. Ren R, Yang P, Han GY (1999) DNA cleavage by copper(II) complexes without added coreactants. Chin Chem Lett 10:383–386